J|A|C|S
ARTICLES
Published on Web 05/26/2005

Three-Dimensional Structure of Nanocomposites from Atomic Pair Distribution Function Analysis: Study of Polyaniline and (Polyaniline)$_{0.5}V_2O_5 \cdot 1.0H_2O$

Valeri Petkov,*,† Vencislav Parvanov,† Pantelis Trikalitis,‡ Christos Malliakas,‡ Tom Vogt,§ and Mercouri G. Kanatzidis*,‡

Contribution from the Department of Physics, Central Michigan University, Mt. Pleasant, Michigan 48859, Department of Chemistry, Michigan State University, East Lansing, Michigan 48824, and Department of Physics, Brookhaven National Laboratory, Upton, New York 11973

Received March 2, 2005; E-mail: petkov@phy.cmich.edu; kanatzidis@chemistry.msu.edu

Abstract: The three-dimensional structures of emeraldine base polyaniline (PANI) and (polyaniline)$_{0.5}V_2O_5 \cdot 1.0H_2O$ have been determined by total X-ray scattering experiments. Atomic pair distribution functions (PDF) were measured to obtain experimental observables against which structural models were tested and refined. The PDF approach is necessary because of the limited structural coherence in these nanostructured materials. Polyaniline possesses a well-defined local atomic arrangement that can be described in terms of an 84-atom orthorhombic unit cell. The nanocomposite (PANI)$_{0.5}V_2O_5 \cdot 1.0H_2O$ too is locally well ordered and may be described in terms of a small number of structure-sensible parameters. The PDF approach allows the construction of structure models of PANI and (PANI)$_{0.5}V_2O_5 \cdot 1.0H_2O$ on the basis of which important materials' properties can be explained predicted and possibly improved.

Introduction

In recent years, conducting polymeric nanocomposites have attracted much attention because of their unique and novel properties and a wide variety of potential applications.[1−5] Of particular interest are nanocomposites based on polyaniline (PANI) which are being investigated for applications in solar cells, biosensors, and color displays.[6−10] A prime example of the family of PANI-based nanocomposites is (PANI)$_xV_2O_5 \cdot nH_2O$.[11] Here the combination of the conducting properties of PANI and the inorganic host, $V_2O_5 \cdot nH_2O$ xerogel, results in a nanomaterial with interesting charge- and ion-transport characteristics.[11,12] No simulations or theoretical studies of the physical properties of these materials have been done thus far, mainly because their nanocrystalline state made it difficult to determine the atomic-scale structure in detail. This difficulty stems from the fact that materials constructed at the nanoscale, such as nanocomposites and polymers, lack the 3D periodicity and translational order of conventional crystals and exhibit very diffuse diffraction patterns with few Bragg peaks. This renders the traditional techniques of structure determination from powder diffraction data, such as Rietveld refinement, inapplicable. Here we show that the atomic-scale structure of complex nanocomposites may be determined using the atomic pair distribution function (PDF) technique. This nontraditional but very promising experimental approach takes into account both Bragg and diffuse scattering and yields the atomic structure in terms of a small set of parameters such as a unit cell and atomic coordinates.[13−17]

The (PANI)$_xV_2O_5 \cdot nH_2O$ system is composed of two components neither of which exists in a crystalline form. The $V_2O_5 \cdot nH_2O$ xerogel is nanocrystalline in nature, and its structure was

† Central Michigan University.
‡ Michigan State University.
§ Brookhaven National Laboratory.

(1) Matsubara, I.; Hosono, K.; Murayama, N.; Shin, W.; Izu, N. *Bull. Chem. Soc. Jpn.* **2004**, *77*, 1231−1237.
(2) Ray, S. S.; Okamoto, M. *Prog. Polym. Sci.* **2003**, *28*, 1539−1641.
(3) Leroux, F.; Besse, M. *Chem. Mater.* **2001**, *13*, 3507−3515.
(4) Wu, C. G.; Chung, H. *J. Solid State Chem.* **2004**, *77*, 2285−2294.
(5) Zeh, J. M.; Liou, S. J.; Lai, C. Y.; Wu, P. C. *Chem. Mater.* **2001**, *13*, 1131−1136.
(6) Wu, J.; Zou, Y. H.; Li, H. L.; Shen, G. L.; Yu, R. Q. *Sensors Actuators B* **2005**, *104*, 43−49.
(7) Dixit, V.; Misra, S. C. K.; Sharma, B. S. *Sensors Actuators B* **2005**, *104*, 90−93.
(8) Enomoto, H.; Takai, H.; Ozaki, H.; Lerner, M. M. *J. Phys.: Condens. Matter* **2005**, *16*, 6375−6384.
(9) Tan, S. H.; Zhai, J.; Wan, M. X.; Meng, Q. B.; Li, Y. L.; Jiang, L.; Zhu, D. B. *J. Phys. Chem. B* **2004**, *108*, 18693−18697.
(10) DeLongchamp, D. M.; Hammond, P. T. *Chem. Mater.* **2004**, *16*, 4799−4805.
(11) Wu, C.-G.; DeGroot, D. C.; Marcy, H. O.; Schindler, J. L.; Kannewurf, C. R.; Liu, Y.-J.; Hirpo, W.; Kanatzidis, M. G. *Chem. Mater.* **1996**, *8*, 1992−2004; Kanatzidis, M. G.; Wu, C. G.; Ho, M.; Kannewurf, C. R. *J. Am. Chem. Soc.* **1989**, *111*, 4139−4141.
(12) Leroux, F.; Koene, B. E.; Nazar, L. F. *J. Electrochem. Soc.* **1996**, *143*, L181−L183.
(13) Gateshki, M.; Hwang, S.-Ju.; Park, D. H.; Ren, Y.; Petkov, V. *Chem. Mater.* **2004**, *16*, 5153−5157.
(14) Petkov, V.; Zavalij, P. Y.; Lutta, S.; Whittingham, M. S.; Parvanov, V.; Shastri, S. *Phys. Rev. B* **2004**, *69*, 085410−085416.
(15) Petkov, V.; Billinge, S. J. L.; Vogt, T.; Ichimura, A. S.; Dye, J. L. *Phys. Rev. Lett.* **2002**, *89*, 075502−075504.
(16) Petkov, V.; Bozin, E.; Billinge, S. J. L.; Vogt, T.; Trikalitis, P.; Kanatzidis, M. *J. Am. Chem. Soc.* **2002**, *124*, 10157−10162.
(17) Billinge, S. J. L.; Kanatzidis, M. G. *Chem. Commun.* **2004**, *7*, 749−760.

unknown ever since the material was discovered in the beginning of the last century. Recently, we determined its atomic-scale structure[16] using the only technique currently available that can do so, namely the PDF technique.[17] Polyaniline is a poorly crystalline material whose three-dimensional structure has not been determined in detail. Here we build upon our previous results and the capabilities of the PDF technique to elucidate the structure of polyaniline itself and that of its nanocomposite. To the best of our knowledge this is the first structural study and structure determination of a poorly crystalline nanocomposite such as $(PANI)_xV_2O_5{\cdot}nH_2O$. We find that the local atomic ordering in PANI is effectively described in terms of polymeric chains made up of four monomer units and its medium-range order is characterized by an intermolecular packing of such chains according to the rules of a (pseudo)orthorhombic lattice. We determine the parameters of the lattice, including the values of the unit cell and the coordinates of the atoms in it, and use them together with our previous structural data for $V_2O_5{\cdot}nH_2O$ (here $n \approx 1.6$) xerogel to build a structural model for one representative of the $(PANI)_xV_2O_5{\cdot}nH_2O$ family—namely $(PANI)_{0.5}V_2O_5{\cdot}1.0H_2O$. The model confirms that the nanocomposite has a lamellar-type structure wherein PANI chains are sandwiched between double layers of $V-O_6$ octahedra. The PDF analysis presented here proves the topotactic nature of PANI insertion into the $V_2O_5{\cdot}nH_2O$ matrix and explains well the observed anisotropy in the material's morphology as well as allows us to understand better the important properties such as the charge transport.

Experimental Section

Sample Preparation. Preparation of the $(PANI)_{0.5}V_2O_5{\cdot}1.0H_2O$ nanocomposite has been described in full detail.[11,18] Here are some of the major steps in the synthetic route employed: $V_2O_5{\cdot}nH_2O$ xerogel was prepared using an aqueous HVO_3 solution as a precursor. The aqueous solution was allowed to polymerize into a V_2O_5 sol for 24−96 h, poured onto glass substrates, and dried into a $V_2O_5{\cdot}1.6H_2O$ gel by letting excess water evaporate in air. The dry gel was peeled off the substrate and ground to a powder for subsequent use. The nanocomposite was obtained by mixing $V_2O_5{\cdot}1.6H_2O$ powder and aniline in water, followed by rigorous stirring at room temperature for 16 h in air. The black powder was isolated by filtration, washed with acetone, and dried in a vacuum. By changing the aniline/V_2O_5 ratio and solvent amount $(PANI)_xV_2O_5{\cdot}nH_2O$ nanocomposites with different stoichiometries can be obtained.[11] The nanocomposite we investigated had the chemical formula: $(PANI)_{0.5}V_2O_5{\cdot}1.0H_2O$. To determine the structure of $(PANI)_{0.5}V_2O_5{\cdot}1.0H_2O$ nanocomposite we had to investigate the structure of three other materials: crystalline V_2O_5, nanocrystalline $(NH_4)_{0.5}V_2O_5{\cdot}0.9H_2O$, and pure polyaniline. Crystalline V_2O_5 and polyaniline (emeraldine base; $(C_6H_4-NH-C_6H_4-NH)_{1-x}(C_6H_4-N{=}C_6H_4{=}N)_x$) were obtained from Aldrich; $(NH_4)_{0.5}V_2O_5{\cdot}0.9H_2O$ was obtained as described in ref 18. All samples were gently ground into fine powder and sealed between Kapton foils for synchrotron radiation scattering experiments.

Synchrotron Radiation Experiments. X-ray diffraction (XRD) experiments were carried out at the beamline ×7a at the National Synchrotron Light Source at Brookhaven National Laboratory using X-rays of energy 29.09 keV ($\lambda = 0.4257$ Å) at room temperature. The higher-energy X-rays were used to obtain diffraction data to higher values of the wave vector, Q, which is important for the success of PDF analysis. The experiments were carried out in a symmetric transmission geometry, and the samples were rocked during the measurements. This experimental style is usually employed to eliminate the preferred sample orientation effect, and we have already successfully applied it in several diffraction studies on layered and fibrous materials.[14,16,18] The scattered radiation was collected with an intrinsic germanium detector connected to a multichannel analyzer. Several runs were conducted with each of the samples, and the resulting XRD patterns were averaged to improve the statistical accuracy and reduce any systematic effects due to possible instabilities in the experimental setup. The diffraction patterns obtained are shown in Figure 1. As can be seen, the XRD pattern of V_2O_5 exhibits well-defined Bragg peaks up to $Q \approx 10$ Å^{-1}. The material is obviously a well-ordered crystalline solid. In contrast, the Bragg peaks in the XRD patterns of nanocrystalline $(PANI)_{0.5}V_2O_5{\cdot}1.0H_2O$ and $(NH_4)_{0.5}V_2O_5{\cdot}0.9H_2O$ are rather broad and merge into a slowly oscillating diffuse component already at Q values as low as 4−5 Å^{-1}. The diffraction pattern of polyaniline is even less structured: it shows only one sharp feature at low Q values—a behavior typical for severely disordered materials. Such diffraction patterns are very difficult to analyze using ordinary techniques for structure determination. However, when reduced to the corresponding atomic PDFs, they become a structure-sensitive quantity lending itself to structure determination and modeling.

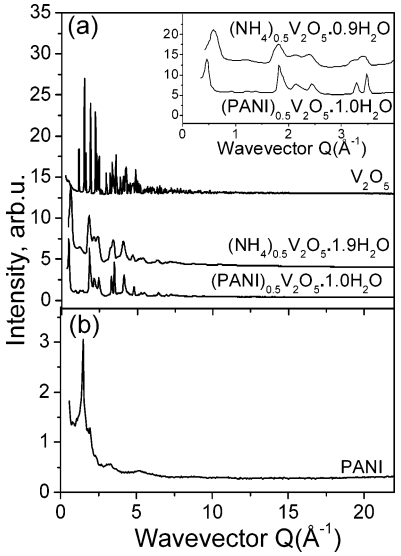

Figure 1. Diffraction patterns of (a) nanocrystalline $(PANI)_{0.5}V_2O_5{\cdot}1.0H_2O$, $(NH_4)_{0.5}V_2O_5{\cdot}0.9H_2O$ and crystalline V_2O_5 and (b) polyaniline. The low-Q parts of the diffraction patterns of nanocrystalline $(PANI)_{0.5}V_2O_5{\cdot}1.0H_2O$ and $(NH_4)_{0.5}V_2O_5{\cdot}0.9H_2O$ are given in the insert in (a) on an expanded scale.

The reduced atomic pair distribution function, $G(r)$, is defined as follows:

$$G(r) = 4\pi r[\rho(r) - \rho_0] \quad (1)$$

where $\rho(r)$ and ρ_0 are the local and average atomic number densities, respectively, and r is the radial distance. It peaks at characteristic distances separating pairs of atoms and thus reflects the atomic-scale structure. The PDF $G(r)$ is the Fourier transform of the experimentally observable total structure function, $S(Q)$, i.e.,

$$G(r) = (2/\pi)\int_{Q=0}^{Q_{max}} Q[S(Q) - 1]\sin(Qr)\mathrm{d}Q \quad (2)$$

where Q is the magnitude of the wave vector ($Q = 4\pi \sin\theta/\lambda$), 2θ is the angle between the incoming and scattered radiation beams, and λ is the wavelength of the radiation used. The structure function is related to the coherent part of the total intensity

(18) Trikalitis, P. N.; Petkov, V.; Kanatzidis, M. G. *Chem. Mater.* **2003**, *15*, 3337−3342.

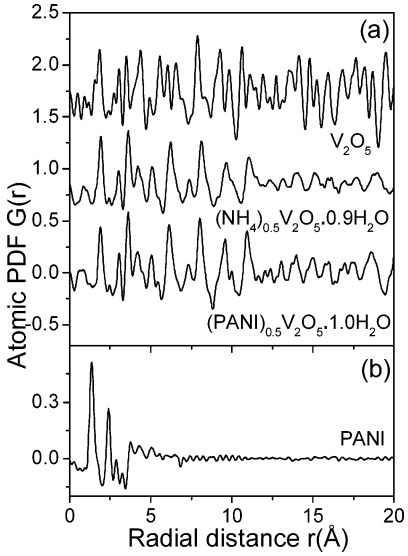

Figure 2. Experimental atomic PDFs for (a) crystalline V_2O_5, nanocrystalline $(PANI)_{0.5}V_2O_5 \cdot 1.0H_2O$ and $(NH_4)_{0.5}V_2O_5 \cdot 0.9H_2O$ and (b) polyaniline. All are derived from the diffraction data of Figure 1.

diffracted from the material as follows:

$$S(Q) = 1 + \frac{[I^{coh}(Q) - \sum c_i |f_i(Q)|^2]}{|\sum c_i f_i(Q)|^2} \quad (3)$$

where $I^{coh}(Q)$ is the coherent scattering intensity per atom in electron units and c_i and f_i are the atomic concentration and X-ray scattering form factor, respectively, for the atomic species of type i.[19,20] As can be seen from eqs 1−3, the PDF is simply another representation of the powder diffraction data. However, exploring the diffraction data in real space is advantageous, especially in the case of materials of limited structural coherence. First, as eq 2 implies, the *total* scattering, including Bragg scattering as well as diffuse scattering, contributes to the PDF. Therefore, both the longer-range atomic structure, responsible for the sharp Bragg-like diffraction features, and the local nonperiodic structural imperfections, resulting in the diffuse component of the diffraction pattern, are contained in the PDF. Second, by accessing high values of Q, experimental PDFs with improved real-space resolution can be obtained, and hence, quite fine structural features can be revealed.[21] In fact, data at high Q values ($Q > 10$ Å^{-1}) are critical to the success of PDF analysis. Third, the PDF is less affected by diffraction optics and experimental factors since these are accounted for when extracting the coherent intensities from the raw diffraction data. This renders the PDF a structure-dependent quantity that gives directly relative positions of atoms in materials and enables convenient testing and refinement of structural models. Experimental PDFs for the samples studied were obtained as follows. First, the coherently scattered intensities were extracted from the XRD patterns shown in Figure 1 by applying appropriate corrections for flux, background, Compton scattering, and sample absorption. The intensities were normalized in absolute electron units, reduced to structure functions $Q[S(Q) - 1]$ and then Fourier transformed to atomic PDFs. Such obtained experimental atomic PDFs are shown in Figure 2. All data processing was done with the help of the program RAD.[22]

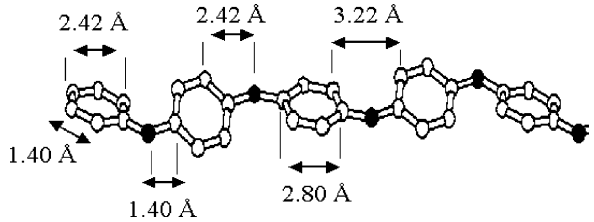

Figure 3. Fragment of a $([C_6H_4-NH-C_6H_4-NH)_{1-x}(C_6H_4-N=C_6H_4=N)_x]$ chain (emeraldine base) showing a set of first, second, third, and fourth atomic neighbor distances. These interatomic distances are seen as four sharp peaks in the experimental atomic PDF for polyaniline shown in Figure 2b. (○) Carbon atoms; (●) nitrogen atoms. Hydrogen atoms are not shown for the sake of clarity.

Results

The atomic PDF for crystalline V_2O_5 shows a series of sharp peaks reflecting the repetitive pattern of well-ordered coordination spheres present in this material (see Figure 2). As we have demonstrated in previous work[16] this experimental PDF may be entirely fitted by the well-known 14-atom unit cell of V_2O_5. The fit yields structural data for V_2O_5 such as a symmetry, unit cell, and atomic coordinates in very good agreement with literature values, thus documenting the fact that atomic PDFs provide a reliable quantitative basis for structure determination.

The peaks in the atomic PDFs for $(PANI)_{0.5}V_2O_5 \cdot 1.0H_2O$ and $(NH_4)_{0.5}V_2O_5 \cdot 0.9H_2O$ are broader and decay in amplitude faster that those in the PDF for crystalline V_2O_5, reflecting the limited degree of structural coherence in these nanocrystalline materials. As we showed previously,[18] $(NH_4)_{0.5}V_2O_5 \cdot 0.9H_2O$ may be described as a stack of double layers of $V-O_6$ octahedra separated by water molecules and ammonium ions. The similarity between the experimental PDFs for $(PANI)_{0.5}V_2O_5 \cdot 1.0H_2O$ and $(NH_4)_{0.5}V_2O_5 \cdot 0.9H_2O$ (see Figure 2a) indicates that these nanocrystalline materials share many common structural features. However, distinct differences are also visible. The first peak in the XRD pattern for $(NH_4)_{0.5}V_2O_5 \cdot 0.9H_2O$ appears at a higher wave vector than the first peak in the XRD pattern for $(PANI)_{0.5}V_2O_5 \cdot 1.0H_2O$ does (see the inset in Figure 1a). This peak position reflects the longer distance between the $V-O_6$ bilayers which are separated more (∼13.6 Å) in the material intercalated with PANI than in that with ammonium ions (∼9.1 Å). This observation shows that the inorganic V_2O_5 matrix expands upon intercalation with PANI in what is known to be a topotactic insertion. The experimental PDF for polyaniline shows four relatively sharp peaks in the region from 1 to 3.5 Å, reflecting the first few well-defined interatomic distances within the $([C_6H_4-NH-C_6H_4-NH)_{1-x}(C_6H_4-N=C_6H_4=N)_x]$ chains, followed by an almost featureless tail mostly reflecting the distances between atoms from neighboring polymeric chains. The interatomic distances seen as four sharp peaks in the PDF for PANI are shown in Figure 3. The present experimental PDF is very similar to the one obtained by others,[23] showing that the characteristic structural features of polyaniline do not vary considerably from sample to sample.

There are several previous structural studies on polyaniline and its forms.[23−26] These studies have provided important

(19) Klug, P. H.; Alexander, L. A. *X-ray Diffraction Procedures for Polycrystalline Materials*; Wiley: New York, 1974.
(20) Waseda, Y. *The Structure of Noncrystalline Materials*; McGraw-Hill: New York, 1980.
(21) Petkov, V.; Jeong, I.-K.; Chung, J. S.; Thorpe, M. F.; Kycia, S.; Billinge, S. J. L. *Phys. Rev. Lett.* **1999**, *83*, 4089−4092.
(22) Petkov, V. *J. Appl. Crystallogr.* **1989**, *22*, 387−390.
(23) Maron, J.; Winokur, M. J.; Mattes, B. R. *Macromolecules* **1995**, *28*, 4475−4486.
(24) Pouget, J. P.; Jozefowicz, M. E.; Epstein, A. J.; Tang, X.; MacDarmid, A. G. *Macromolecules* **1991**, *24*, 779−789.
(25) Winokur, M. J.; Mattes, B. R. *Phys. Rev. B* **1996**, *54*, R12637−R12640.
(26) Baughman, R. H.; Wolf, J. F.; Eckhardt, H.; Shacklette, L. W. *Synth. Met.* **1998**, *25*, 121−137.

qualitative information about the geometrical characteristics of $(C_6H_4-NH-C_6H_4-NH)_{1-x}(C_6H_4-N=C_6H_4=N)_x$ chains and some insight on the interchain packing. Unfortunately, to our best knowledge, a three-dimensional (3D) structural model of polyaniline, including a unit of repetition and coordinates of atoms within it, has not been reported. Such detailed structural information is, however, needed if the atomic ordering in the $(PANI)_{0.5}V_2O_5 \cdot 1.0H_2O$ nanocomposite is to be determined. Thus, we had to solve three problems to find a structure model for $(PANI)_{0.5}V_2O_5 \cdot 1.0H_2O$: (i) determine the 3D structure of polyaniline, (ii) refine the 3D structure of the inorganic V_2O_5 matrix, in particular, find how exactly it expanded due to the intercalation with PANI, and (iii) combine the structural models of PANI and the expanded matrix into one, giving as realistic as possible a description of the atomic ordering in the nanocomposite. All steps in the structural investigation conducted by us, including verifying trial structures, refining plausible structures, and discriminating between competing structural models, were guided by the experimental atomic PDFs for the respective materials.

Discussion

(i) Determining the 3D Structure of Polyaniline. Previous studies have come to the conclusion that the polymeric chains in PANI may be best represented as a repetitive sequence of four monomer units of the C_6H_4-type described by the general chemical formula $(C_6H_4-NH-C_6H_4-NH)_{1-x}(C_6H_4-N=C_6H_4=N)_x$.[23−26] A fragment of such a chain, including the four repetitive monomer units, is shown in Figure 3. Polymeric chains in PANI have been found to be not quite planar with some of the individual monomer units nearly perpendicular to the nominal molecular plane,[23−26] where the nominal plane is the one that would accommodate all atoms from a chain if it were fully planar. While the atomic ordering within the chains seems to be relatively well understood, the interchain arrangement and packing in PANI are still an open question. On the basis of limited diffraction data it has been suggested that the extended order in PANI and its salts may be described in terms of an orthorhombic unit cell whose longest edge runs in parallel with the individual chains while the other two edges have zero and 90° angles with the nominal molecular plane, respectively.[24]

The same studies have identified two different forms of the emeraldine base state of polyaniline, EB-I and EB-II, and two forms of the corresponding semicrystaline salts, ES-I and ES-II.[24] The atomic ordering in all PANI forms is suggested to bear similar characteristics. The major difference between EB-I and EB-I is the degree of their crystallinity,[24] and that between ES-I and ES-II is the relative positioning of the chains with respect to each other, referred to as a "phase difference".[24] Here we concentrate on finding a model for the emeraldine base form of PANI with a minimal complexity but still capable of describing all essential features of its local structure. Such a model may be used as a realistic basis for building extended atomic configurations with different degrees of crystallinity (e.g., EB-I, EB-II) and/or reduced dimensionality (e.g. 2D in cases when PANI is inserted in an inorganic matrix).

We started with a model based on a single PANI chain of four monomer units inside an orthorhombic unit cell as in previous studies.[23,25] For the sake of simplicity we considered the monomer $-C_6H_4-$ units to be of the same benzenoid type (i.e. we ignored the fact that one of the four monomers shows quinoidal distortions). Also, we ignored all hydrogen atoms since their contribution to the experimental PDFs is negligible due to the low scattering power of hydrogen for X-rays. In line with previous modeling studies we kept the monomer units rigid and adjusted only their relative orientation with respect to each other (i.e. adjusted the dihedral angles) so as to obtain as good as possible an agreement between the experimental and calculated atomic PDFs. Furthermore, we adjusted the parameters of the unit cell and the degree of chain packing to approach as close as possible the experimental atomic density:[24] 1.3−1.4 g/cm^3. The corresponding atomic PDF is shown in Figure 4a. As can be seen the model reproduces relatively well the first three sharp peaks in the experimental data, i.e. it reproduces well the intrachain atomic correlations in PANI. However, it fails to reproduce the continuum of longer-range (longer than 3.4 Å) interchain atomic correlations.

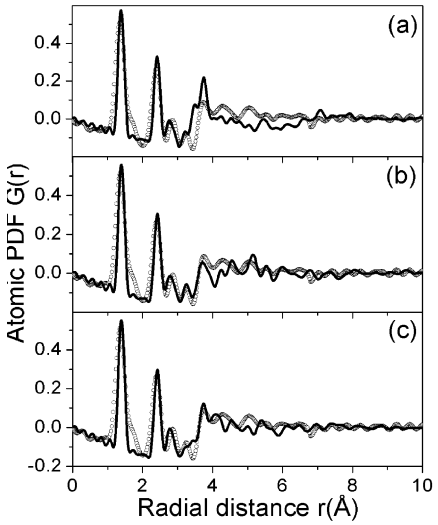

Figure 4. Comparison between the experimental PDF for polyaniline (symbols) and model PDFs calculated from atomic configurations based on (a) one, (b) two, and (c) three individual PANI chains per unit cell as described in the text.

Next, we considered a model based on two PANI chains each with its own internal degrees of freedom (dihedral angles). The relative position of the two chains with respect to each other and the parameters of the unit cell enclosing the chains were adjusted to reproduce the experimental density and obtain as close as possible an agreement with the experimental PDF data. The corresponding atomic PDF is shown in Figure 4b. The model performed better but still could not reproduce the longer-range part of the experimental PDF, i.e. the interchain packing in PANI.

In the next trial model we considered three PANI chains. The model showed good promise as can be seen in Figure 4c, indicating that at least three independent chains are necessary to describe the essential structural features of PANI. The geometrical characteristics of each of the three chains, their relative positions (i.e., packing), and the parameters of the orthorhombic unit cell were varied independently until the most important details in the experimental PDF were well reproduced as can be seen in Figure 5. Given the high degree of disorder inherent in PANI, the level of agreement achieved is quite satisfactory and acceptable.

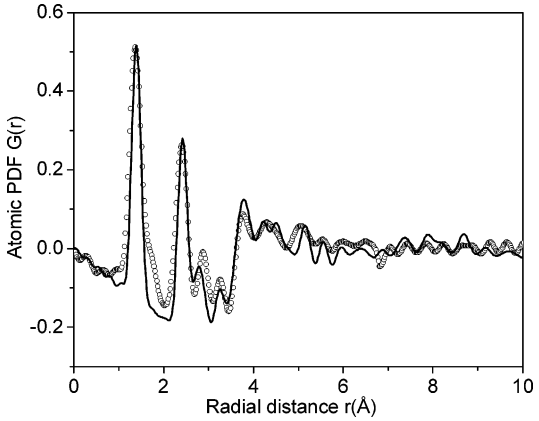

Figure 5. Comparison between the experimental (○) and model (—) PDFs for polyaniline. The model PDF is calculated from the configuration shown in Figure 6. The high-frequency ripple in the experimental data at low values and the weak shoulders at both sides of the first PDF peak are due to termination and experimental errors that may not be reproduced by our model of PANI.

The orthorhombic periodic cell of the refined model is shown in Figure 6 in three different projections. The parameters of the model including the unit cell constants ($a = 20.317$ Å, $b = 10.9$ Å, $c = 5.2$ Å, $\alpha = \beta = \gamma = 90°$) and the coordinates of the atoms in it (84 atoms in total) are available as Supporting Information (as a file in CIF format). The analysis of the model structure shows that its characteristic features such as C−C, C−N, N−N distances and dihedral angles are quite close to those found in other independent structural studies on PANI.[23−26]

It should be mentioned that previous modeling studies have relied on a single polymeric chain and have treated the intra- and interchain atomic correlations in a substantially different manner, assuming the presence of a relatively small degree of disorder within the chains and a much larger one between them. We have adopted a more realistic approach by treating the intra- and interchain atomic distances the same way as separations between atoms showing the usual root-mean-square fluctuations, u, ($u_C = u_N = 0.14$ Å in our model for PANI) around their average positions. That is why our model needed three independent polymeric chains and not one to take into account all essential structural features of the PDF of PANI. Also, previous studies[24] have suggested two possible arrangements of the polymeric chains in polyaniline, staggered (see Figure 10b in ref 24) and eclipsed (see Figure 12b in ref 24). All our models based on this staggered-type arrangement did not perform well. The one we propose features the polymeric chains in an eclipsed-type arrangement similar to the one suggested for the EB-I form of polyaniline.

(ii) Refining the Structure of the V_2O_5 Inorganic Host. Given the similarities between the experimental PDFs for $(NH_4)_{0.5}V_2O_5{\cdot}0.9H_2O$ and $(PANI)_{0.5}V_2O_5{\cdot}1.0H_2O$, we considered the structure of the former as a starting model for that of the PANI-intercalated material. As we showed in previous work[18] the structure of $(NH_4)_{0.5}V_2O_5{\cdot}0.9H_2O$ features V_2O_5 bilayers stacked along the c axis of a monoclinic unit cell (space group $C2/m$) with parameters $a = 11.845$ Å, $b = 3.677$ Å, and $c = 9.058$ Å and $\beta = 88.635°$. To account for the fact that the interlayer distance in $(PANI)_{0.5}V_2O_5{\cdot}1.0H_2O$, as measured by the position of the first Bragg peak in the XRD pattern, is ∼13.6 Å we increased the c parameter of the unit cell from 9.058 to 13.6 Å and adjusted the z coordinates of V and O atoms accordingly. The interlayer space was considered empty.

The constructed model takes into account only the more structurally ordered, inorganic part of the essentially two-component nanomaterial, and as such it may yield structural parameters good to a first approximation only. Nevertheless, these parameters are necessary as input in the subsequent joint structure refinement of the two components of $(PANI)_{0.5}V_2O_5{\cdot}1.0H_2O$. This initial model was refined against the atomic PDF for $(PANI)_{0.5}V_2O_5{\cdot}1.0H_2O$ over the region of r values from 1.6 to 20 Å where all sharp features in the experimental data are located. In the refinement the constraints of the space group $C2/m$ were strictly observed. The program PDFFIT[27] was used to carry out the calculations. The program employs a least-squares procedure to compare experimental and model data (PDF) calculated from a plausible structural model. The structural parameters of the model (unit cell constants, atomic coordinates, and thermal factors) are adjusted until the best possible fit to the experimental data is achieved. The progress of the refinement is assessed by computing an agreement factor, R_w:

$$R_w = \left\{ \frac{\sum w_i (G_i^{\,\mathrm{exp}} - G_i^{\,\mathrm{calc}})^2}{\sum w_i (G_i^{\,\mathrm{exp}})^2} \right\}^{1/2} \qquad (4)$$

where G^{exp} and G^{calc} are the experimental and calculated PDFs, respectively, and w_i are weighting factors reflecting the statistical quality of the individual data points. Thus refined structural parameters of the V_2O_5 matrix are summarized in Table 1. A comparison between the corresponding model and experimental PDFs is given in Figure 7a. As can be seen in this figure the inorganic matrix is more structurally ordered than the intercalated organic component and determines the general shape and positions of most peaks in the experimental PDF for $(PANI)_{0.5}V_2O_5{\cdot}1.0H_2O$ nanocomposite. The residual between the fit and experiment is due to the unaccounted correlations between the atoms in PANI and those between PANI and the V_2O_5 matrix. It is a slowly varying function as one might expect considering the greatly disordered state of PANI. A realistic model for $(PANI)_{0.5}V_2O_5{\cdot}1.0H_2O$ should minimize this residual as well as the corresponding integral quantity, the agreement factor R_w, and this was the focus in the next step of our structural investigation.

(iii) Determining the Structure of the $(PANI)_{0.5}V_2O_5{\cdot}1.0H_2O$ Nanocomposite. To assess in greater detail how the PANI and $V_2O_5{\cdot}nH_2O$ components mix at the atomic level, we considered several models based on the structures of PANI and V_2O_5 matrix discussed above. We did not consider the small amount of water present in the nanocomposite material due to

(27) Proffen, T.; Billinge, S. J. L. *J. Appl. Crystallogr.* **1999**, *32*, 572−575.
(28) It may be noted that the agreement factors achieved with the PDF refinements often appear somewhat high when compared to those resulting from the Rietveld refinement of diffraction data in reciprocal space. This does not indicate an inferior structure refinement but merely reflects the fact that the atomic PDF being fit differs from the corresponding XRD pattern and is a quantity much more sensitive to local ordering in materials. As a result, R_w's greater than 20% are common with PDF refinements even of well-crystallized materials.[13−18] The inherently higher absolute value of the goodness-of-fit factors resulting from PDF-based refinements does not affect their functional purpose as a residuals quantity that must be minimized to find the best fit and as a quantity allowing differentiation between competing structural models.

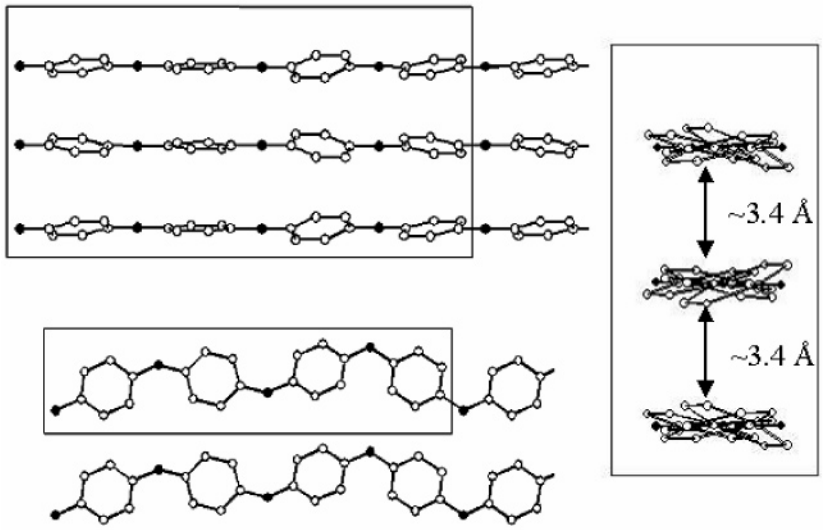

Figure 6. Atomic arrangement in bulk polyaniline projected along the different edges of the orthorhombic unit cell (outlined with thin solid lines) as determined by the present PDF studies. (●) Nitrogen atoms; (○) carbon atoms. Hydrogen atoms are not shown for the sake of clarity. The corresponding model PDF is shown in Figure 5.

Table 1. Positions of the Atoms in the Unit Cell of V_2O_5 Matrix of $(PANI)_{0.5}V_2O_5 \cdot 1.0H_2O$ as Determined by the Present PDF Studies

atomic species	*X* coordinate	*Z* coordinate
V1	0.920	0.095
V2	0.218	0.110
O1	0.380	0.130
O2	0.083	0.055
O3	0.735	0.060
O4	0.930	0.238
O5	0.200	0.250

[a] The space group is *C*2/*m* and the unit cell parameters are $a = 11.66$ Å, $b = 3.64$ Å, $c = 13.65$ Å and $\beta = 86.41°$. The *Y* coordinate of all atoms is zero.

the almost negligible contribution of the former to the diffraction data. The same simplification was made in our successful structure study on $(NH_4)_{0.5}V_2O_5 \cdot 0.9H_2O$.[18] The models of PANI-based nanocomposites were constructed by inserting fragments of PANI chains into the open space between the V_2O_5 bilayers in such a way that the structural integrity of either component was not destroyed. Our reasoning behind this approach was based on the facts that: (i) the V_2O_5 bilayers are well preserved in $(PANI)_{0.5}V_2O_5 \cdot 1.0H_2O$ as our and other previous[11] studies show (topotactic intercalation), (ii) the polymer extracted from the $(PANI)_{0.5}V_2O_5 \cdot 1.0H_2O$ nanocomposite was found[11] to be essentially PANI but with a lower than usual molecular weight reflecting the shorter length of the polymeric chains formed in the structurally restricted interlayer space of the V_2O_5 matrix. Also, in inserting PANI chains into the inorganic matrix, care was taken not to create unrealistically close polymer−matrix interatomic distances.

First we considered models in which the nominal plane of the PANI chains and V_2O_5 bilayers were parallel to each other. Two such models, one representing a stack of two, and the other, of three PANI chains sandwiched between V_2O_5 bilayers, are shown in Figure 8a and b, respectively. The stacks of PANI chains were moved laterally to maximize the agreement between the model and experimental PDF data. The model PDFs corresponding to the best agreement obtained are shown in Figure 9a and b, respectively. As can be seen the models featuring $(PANI)_{0.5}V_2O_5 \cdot 1.0H_2O$ as an assembly of PANI

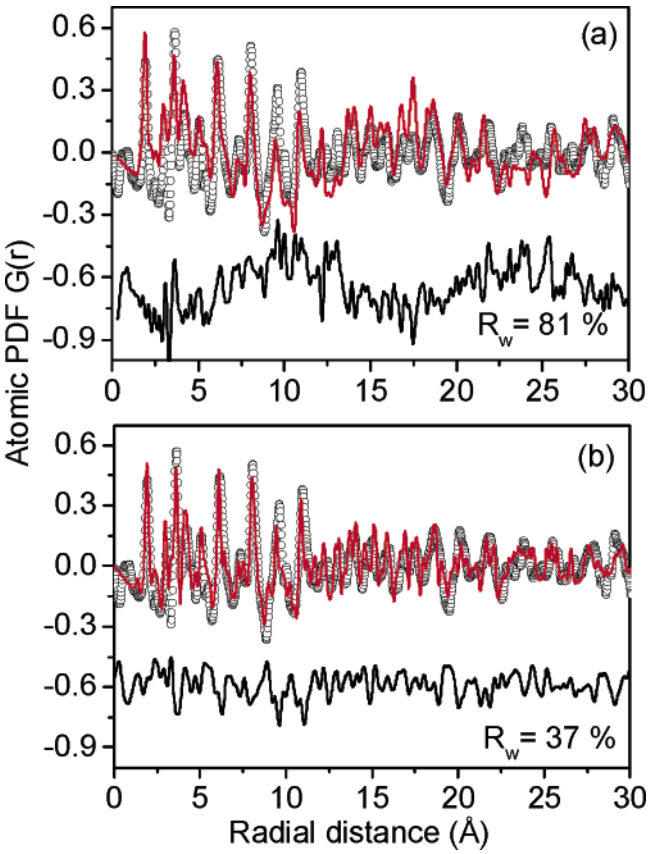

Figure 7. Comparison between the experimental PDF for $(PANI)_{0.5}V_2O_5 \cdot 1.0H_2O$ (○) and model PDFs (— in red) for (a) vanadium pentoxide xerogel without PANI and (b) with PANI intercalated between the V_2O_5 layers as shown in Figure 10. The residual difference between the model and experimental data is given in the lower part of the plots, and it is shifted for clarity. The corresponding agreement factors,[28] R_w, are given in the lower part of the plots.

chains and V_2O_5 layers that are parallel to each other (Figure 8a and b) are not able to reproduce the experimental diffraction data to an acceptable level and therefore are ruled out. This conclusion is in line with the considerations made in ref 11.

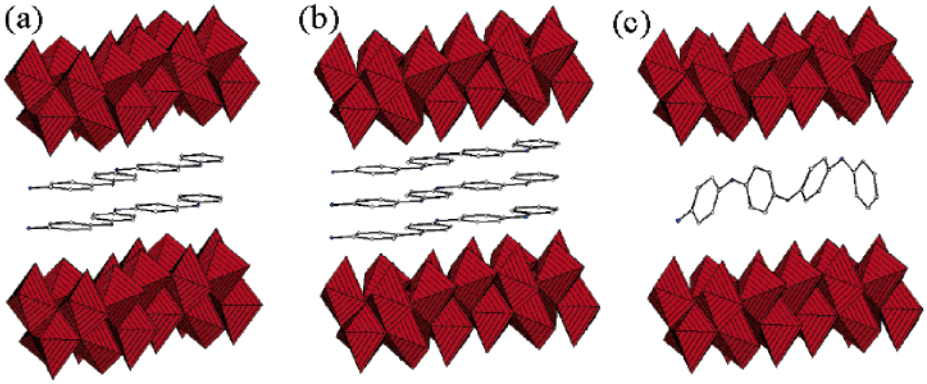

Figure 8. Possible arrangements of PANI chains between V_2O_5 bilayers.

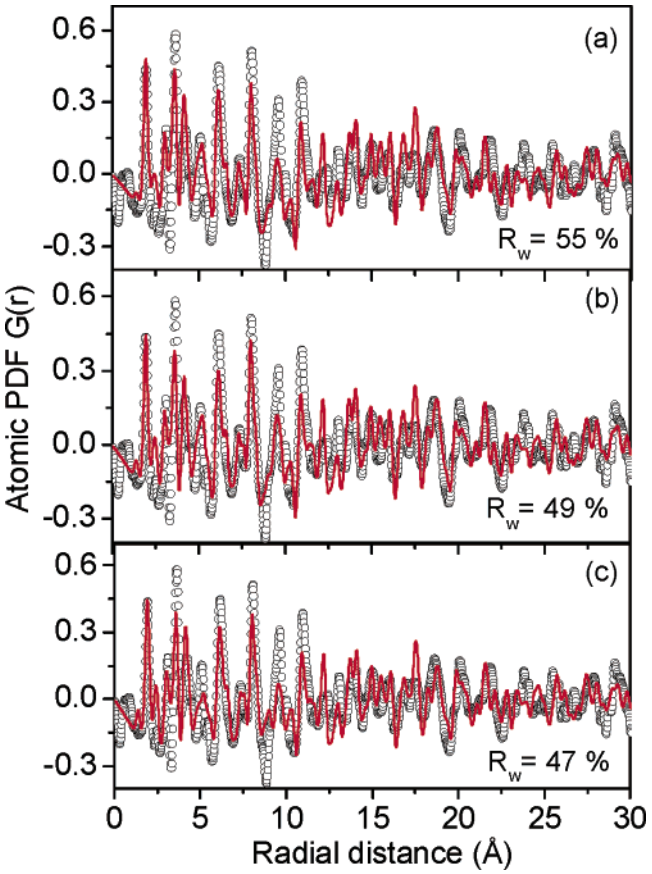

Figure 9. Comparison between the experimental (○) and model (— in red) PDFs for $(PANI)_{0.5}V_2O_5 \cdot 1.0H_2O$. The model PDFs in (a), (b), and (c) are calculated from the atomic configurations shown respectively in parts a, b, and c of Figure 8. The corresponding agreement factors,[28] R_w, are given in the lower part of the plots.

Next we considered models in which the nominal plane of the PANI chains and the V_2O_5 bilayers are perpendicular to each other. Since the inorganic matrix lets the intercalated PANI evolve only in two dimensions, its chains might not be able to pack the way they do in pure PANI. This possibility was explored by constructing a model featuring the nanocomposite as an assembly of V_2O_5 bilayers enclosing space not quite densely populated with PANI chains, i.e., we let the interchain distance in the intercalated PANI to be much longer than that in pure PANI. A fragment of the model is shown in Figure 8c and the corresponding PDF is given in Figure 9c. As can be seen, the model does not perform very well in the region of r values from 5 to 12 Å and was also ruled out as a possibility.

Finally, we considered a model featuring the nanocomposite as an assembly of V_2O_5 bilayers enclosing space containing PANI chains packed as densely, i.e., separated at approximately 3.4 Å, as in pure PANI. Again, when inserting the polymeric chains into the inorganic matrix, care was taken not to create unrealistically close polymer−matrix interatomic distances. In addition, various positions of the stack of chains inside the interlayer space were tested, including positions resulting in the PANI chains being lined up with either the *a* or *b* directions of the monoclinic unit cell describing the inorganic matrix. The PDFs of the test models were compared with the experimental PDF data. The structure refinement was stopped when a model that greatly reduces the residual between the model and experimental data and yields the lowest possible agreement R_w factor, as shown in Figure 7b, was found. A fragment of the corresponding atomic configuration is shown in Figure 10. Structural parameters describing the model, including coordinates of the individual atoms (476 in total), are available as Supporting Information (as a file in Protein Data Bank format). The model is periodic and of relatively small size (given the complexity of the nanomaterial studied) thereby allowing the exploration of structure−property relationships in $(PANI)_{0.5}V_2O_5 \cdot 1.0H_2O$. It describes the nanocomposite as an intimate mix of V_2O_5 bilayers and PANI chains, whose nominal planes are perpendicular to the layers, and corroborates the conclusions drawn in previous studies.[11]

It is likely that the model misses some subtle details of the atomic structure in the nanocomposite such as the likely presence of NH−O−V hydrogen bonding between the PANI chains and the V_2O_5 matrix,[6] a possible "freezing" of some of $-C_6H_4-$ monomers units inside the constrained interlayer space, and a possible presence of stacking faults resulting in PANI chains being separated at distances somewhat longer than 3.4 Å. Therefore, the model should be considered and used with care, bearing in mind that it is still an approximation to the structure of $(PANI)_{0.5}V_2O_5 \cdot 1.0H_2O$. More subtle details as the ones mentioned above may be tested and explored by using structural information provided by local probes and spectroscopic techniques such as EPR, NMR, IR, Raman, etc. This structural level of detail goes beyond the scope of the present work. However, even as an approximation to the real structure of the nanocomposite, the present model is still a major step toward a better understanding of its properties. In particular, the model is capable of explaining the anisotropy in material's morphology. The layered-type character of the local atomic ordering would make it easier for the material to evolve along the layers than

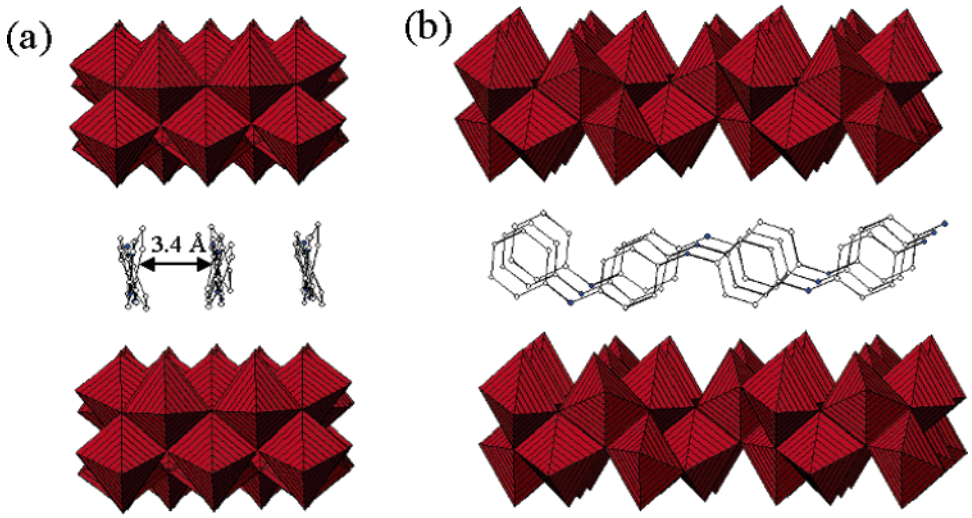

Figure 10. Atomic ordering in $(PANI)_{0.5}V_2O_5 \cdot 1.0H_2O$ as determined by the present PDF studies. Presented are projections along (a) *a* and (b) *b* axis of the monoclinic lattice used to describe the inorganic V_2O_5 matrix.

in a direction perpendicular to the layers. It is thus not a surprise that the nanocomposite exists as sheets as revealed by TEM experiments.[11] The presence of a monolayer of PANI sandwiched between slabs of $V-O_6$ octahedra explains the observed charge transport properties too. They are best described in terms of polaronic conductivity based on small polarons associated with the well-structured inorganic host and much more massive ones located on the constrained PANI chains.[11] Furthermore, the data allow assessment of the performance of the nanocomposite in potential applications. For example, it is reasonable to assume that the rigid and well-structured V_2O_5 matrix imposes an extra degree of longer-range ordering on the PANI chains that is absent in bulk polyaniline. This could facilitate the transport of Li ions through the available interchain galleries (~3.4 Å; see Figure 10) and explain the well-behaved reversible Li charge/discharge process exhibited by $(PANI)_xV_2O_5 \cdot nH_2O$ when used as a cathode battery material.[12]

The results presented here demonstrate how the recent progress in synchrotron radiation sources and computing coupled with the use of a nontraditional experimental approach, such as the PDF technique, make it possible to obtain detailed local structural information about nanocomposite and noncrystalline materials and use it to improve our understanding of their properties. We hope our work will stimulate more investigations of this type.

Conclusion

The three-dimensional structures of the scientifically and technologically important polyaniline and its $(PANI)_{0.5}V_2O_5 \cdot 1.0H_2O$ nanocomposite were determined by the PDF technique. The structures are given in terms of a small number of sensible parameters such as unit cells and coordinates of the atoms in them. This development opens up the route to better explaining, predicting, and possibly improving the properties of these materials by using both theoretical and experimental tools. The results of this work also prove unequivocally that the intercalative polymerization reaction converting $V_2O_5 \cdot nH_2O$ xerogel to $(PANI)_xV_2O_5 \cdot nH_2O$ nanocomposite is indeed topotactic.

The results of the present study are a direct demonstration of the ability of the PDF technique to yield three-dimensional structural information for materials of limited structural coherence, including nanostructured materials and organic/inorganic hybrids. The technique succeeds because it relies on total scattering data obtained from the material and, as a result, is sensitive to its essential structural features regardless of crystalline periodicity. This allows a convenient testing and refining of structural models. Furthermore, the technique probes the bulk and can provide an important foundation to imaging techniques such as transmission electron and atomic force microscopy, which reveal only structural features projected down one axis or a surface.

Acknowledgment. Thanks are due to Y. Lee from BNL for help with the synchrotron radiation experiments. The work was supported by NSF through Grant DMR 0304391(NIRT). Beamline X7a at the NSLS is supported by the U.S. Department of Energy through DE-AC02-98-CH0886.

Supporting Information Available: Structure data for polyaniline (in CIF format) and $(PANI)_{0.5}V_2O_5 \cdot 1.0H_2O$ (in PDB format). This material is available free of charge via the Internet at http://pubs.acs.org.

JA051315N